Demand response potential of aggregated high-temperature storage radiators

Cai, Hanmin; You, Shi; Klyapovskiy, Sergey; Bindner, Henrik W.

Published in:
Journal of Physics: Conference Series

Link to article, DOI:
10.1088/1742-6596/1343/1/012122

Publication date:
2019

Document Version
Publisher's PDF, also known as Version of record

Journal of Physics: Conference Series

PAPER • **OPEN ACCESS**

Demand response potential of aggregated high-temperature storage radiators

To cite this article: Hanmin Cai *et al* 2019 *J. Phys.: Conf. Ser.* **1343** 012122

Demand response potential of aggregated high-temperature storage radiators

Hanmin Cai, Shi You, Sergey Klyapovskiy and Henrik W. Bindner

Department of Electrical engineering, Technical University of Denmark, Elektrovej, 2800 Kgs. Lyngby, Denmark

E-mail: sy@elektro.dtu.dk

Abstract. This study experimentally evaluates the demand response potential of aggregated high-temperature storage radiators to support intermittent solar photovoltaic (PV) production. Nine storage radiators on one floor of an office building located in Copenhagen's Nordhavn area are aggregated. Their demand response potential to compensate for the forecast errors of production from a large-scale PV installation in the same area is analysed. From experimental results, it is found out that the aggregated storage radiators have an activation time of 15 seconds and could provide a significant amount of energy storage while maintaining end-users' comfort.

1. Introduction

As the share of energy production from intermittent renewable energy sources (RES) grows, the needs for energy storage and balancing reserve increase. Thermal energy storage in the residential sector represents one type of low-cost distributed storage [1][2]. Demand response has been widely recognised as one of the techniques to exploit this storage capacity.

Previous studies on thermal storage's demand response potential focus on the thermal inertia of building mass [3]. The commercial buildings' capability of providing frequency regulation has been experimentally demonstrated in [4]. Unidirectional loads have been experimentally validated to be capable of providing frequency normal-operation reserve (FNR) [5], one type of primary frequency regulation service in Denmark, provided that the reference power is set to be half of the total power rating.

This study exploits the high storage capacity from well-insulated high-temperature electric storage radiators and reveals their demand response potential for frequency regulation and other balancing needs. The paper has been organised in the following way. Section 2 presents the methodology adopted in this study. Section 3 summarises the experimental results. Finally, section 4 concludes this paper with remarks on future work.

2. Methodology

The methodology consists of two parts. Firstly, an experimental platform is built to identify thermal dynamics inside the radiator. Secondly, nine storage radiators are aggregated to track external set points received via the communication gateway.

2.1. Experimental platform

Internal structure of an off-the-shelf high-temperature storage radiator is illustrated in Figure 1(a). It is composed of a core, a resistive boost element and a fan. The core is made of high-density magnetite storage cells insulated with micro-porous silica and calcium silicate. It could be heated with a resistive electric heating coil embedded in the core, and it is capable of storing as much as 23.1 kWh of thermal energy. The heating power rating is 3 kW. The boost element of 1.2 kW is mainly used as a backup in freezing weathers. When space heating is requested, the fan circulates hot air into the room with a thermal power rating of 1.5 kW. All these components have built-in thermostats with set points that could be remotely adjusted. Figure 1(b) illustrates the remote control of one storage radiator. A microcontroller uses a universal asynchronous receiver-transmitter (UART) wireless transceiver to communicate with the storage radiator and it could both read temperature measurements and adjust temperature set points. In addition, the microcontroller reads frequency and voltage measurements from the smart meters.

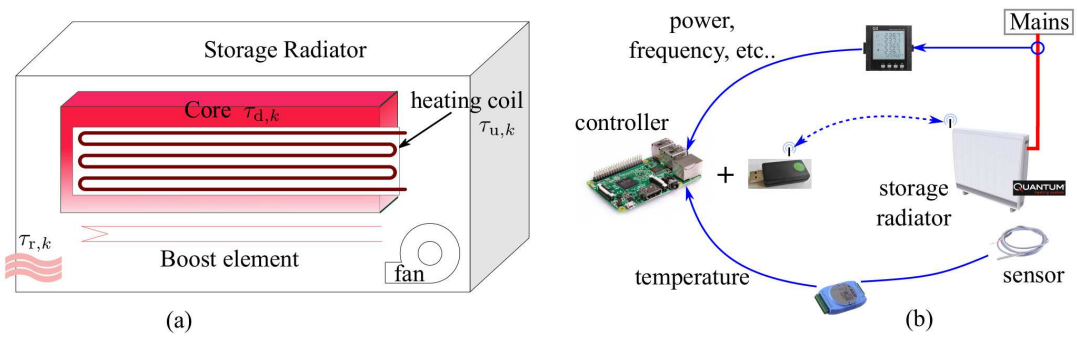

Figure 1: Illustration of wireless control of storage radiator [6]. (a): storage radiator internal structure; (b): control and communication setup

In this study, nine storage radiators on one floor of an office building are aggregated. Two types of storage radiators are used according to the heating needs in different zones. The typical device specifications are summarised in Table 1.

Table 1: Key parameters for the two types of storage radiators used in the experiment

Type 1 parameter	Value	Unit	Type 2 parameter	Value	Unit
Heat output	1.5	kW	Heat output	1	kW
Storage capacity	23.1	kWh	Storage capacity	15.5	kWh
Dimension	0.19/0.73/1.07	m	Dimension	0.16/0.73/0.87	m
Core charge rating	3.02	kW	Core charge rating	2.04	kW
Boost rating	1.24	kW	Boost rating	1.02	kW

The building located in Copenhagen's Nordhavn area is shown in Figure 2 along with a large-scale rooftop solar PV installation and a medium-size electric battery of 460 kWh. The PV installation has an annual electricity production of 200 MWh. While the electric battery is capable of both charging and discharging to support the PV integration with a fast response

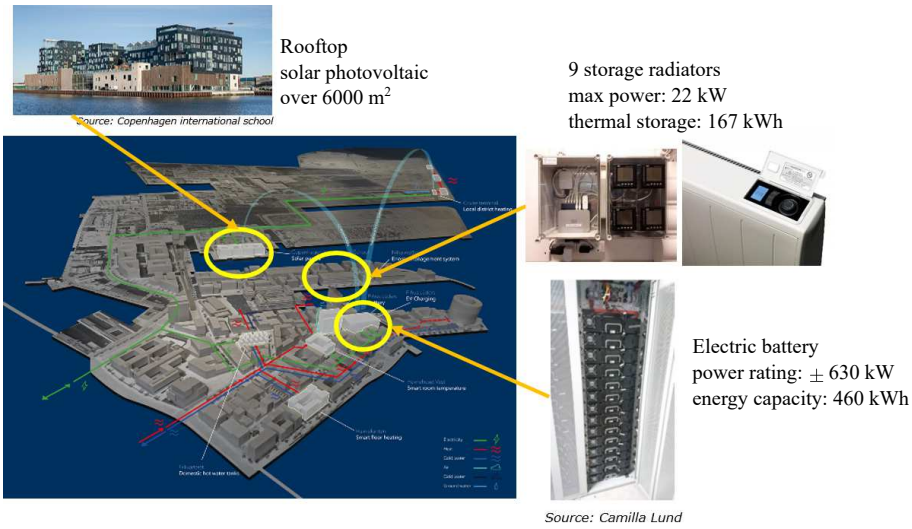

Figure 2: Combine electric battery and thermal storage to compensate for PV production forecast error

rate, it has a relatively low energy capacity, and this could be improved in combination with the storage radiators.

An electric box consisting of a microcontroller, four smart meters and a communication gateway is built to aggregate the nine storage radiators and evaluate their overall response, as shown in Figure 3(a). The microcontroller aggregates the nine storage radiators by sequentially controlling each radiator. The communication gateway allows the microcontroller to receive external aggregate power set points from the PV installation owner and report the aggregated energy storage status. The smart meters' frequency measurements allow the controller to provide frequency regulation autonomously without any external communication. An example of using this platform is given in Figure 3(b), where the core's charging and free cooling processes are shown. The data collected are used for the grey-box modelling of the radiator's dynamics.

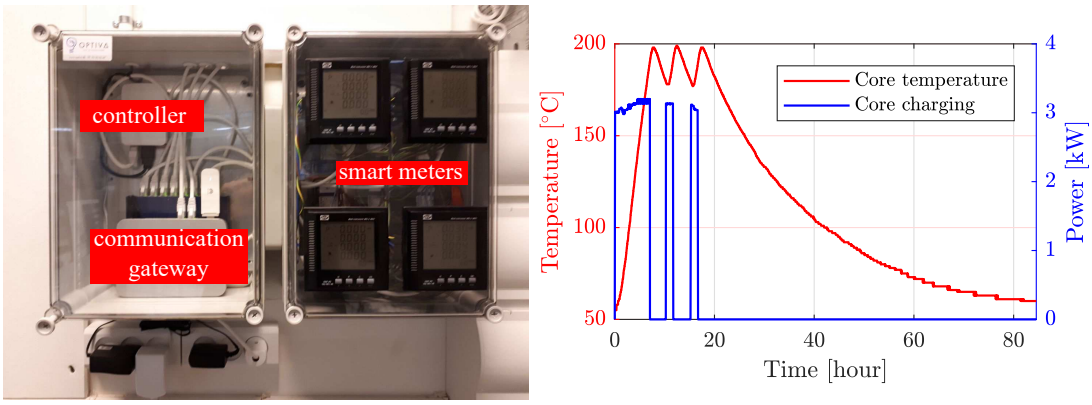

(a) (b)

Figure 3: (a) controller unit supplemented with communication gateway and smart meters; (b) analysis of the core charging and free cooling processes using the experimental platform

2.2. Modelling of core charging

The temperature overshoot after the core charging stops in Figure 3(b) suggests the system dynamics could be of second order. Acknowledging the fact that the temperature is not uniformly distributed, we divide the space inside the radiator into two zones: $\tau_{\mathrm{u},k}$ denotes the temperature at the heating coil and $\tau_{\mathrm{d},k}$ denotes the temperature at the core. In the experimental set up, only one sensor is placed close to the core to measure $\tau_{\mathrm{d},k}$, as illustrated in Figure 1. The energy balance equations for the core is formulated in Eq. (1).

$$c_{\mathrm{d}} m_{\mathrm{d}}(\tau_{\mathrm{d},k+1} - \tau_{\mathrm{d},k}) = U_{\mathrm{d}} A_{\mathrm{d}}(\tau_{\mathrm{r},k} - \tau_{\mathrm{d},k})\Delta t + U_{\mathrm{u}} A_{\mathrm{u}}(\tau_{\mathrm{u},k} - \tau_{\mathrm{d},k})\Delta t \tag{1}$$

where c_{d}, m_{d}, τ_{d}, $U_{\mathrm{d}}A_{\mathrm{d}}$ are the specific heat, mass, temperature of the core and thermal resistance of the insulation; Δt is the time interval between each time step; τ_{r} is the room temperature; c_{u}, m_{u}, τ_{u}, $U_{\mathrm{u}}A_{\mathrm{u}}$ are the specific heat, mass, temperature of the coil and thermal resistance between the coil and the core. Throughout the paper, k is used to represent the time step. Energy balance for the resistive coil could be formulated as in Eq. (2).

$$c_{\mathrm{u}} m_{\mathrm{u}}(\tau_{\mathrm{u},k+1} - \tau_{\mathrm{u},k}) = P_{\mathrm{el},k}\Delta t - U_{\mathrm{u}} A_{\mathrm{u}}(\tau_{\mathrm{u},k} - \tau_{\mathrm{d},k})\Delta t \tag{2}$$

Combining Eq. (1) and Eq. (2) gives Eq. (3).

$$\begin{bmatrix} \tau_{\mathrm{d},k+1} \\ \tau_{\mathrm{u},k+1} \end{bmatrix} = \begin{bmatrix} 1 - \frac{U_{\mathrm{d}}A_{\mathrm{d}}\Delta t}{c_{\mathrm{d}}m_{\mathrm{d}}} - \frac{U_{\mathrm{u}}A_{\mathrm{u}}\Delta t}{c_{\mathrm{d}}m_{\mathrm{d}}} & \frac{U_{\mathrm{u}}A_{\mathrm{u}}\Delta t}{c_{\mathrm{d}}m_{\mathrm{d}}} \\ \frac{U_{\mathrm{u}}A_{\mathrm{u}}\Delta t}{c_{\mathrm{u}}m_{\mathrm{u}}} & 1 - \frac{U_{\mathrm{u}}A_{\mathrm{u}}\Delta t}{c_{\mathrm{u}}m_{\mathrm{u}}} \end{bmatrix} \begin{bmatrix} \tau_{\mathrm{d},k} \\ \tau_{\mathrm{u},k} \end{bmatrix} + \begin{bmatrix} 0 \\ \frac{\Delta t}{c_{\mathrm{u}}m_{\mathrm{u}}} \end{bmatrix} P_{\mathrm{el},k} + \begin{bmatrix} \frac{U_{\mathrm{d}}A_{\mathrm{d}}\Delta t}{c_{\mathrm{d}}m_{\mathrm{d}}} \\ 0 \end{bmatrix} \tau_{\mathrm{r},k} \tag{3}$$

2.3. Modelling of core discharging

The core discharges stored heat by starting the fan to circulate hot air flow into the room. The process could be viewed as a convective heat transfer and the transfer coefficient for the air flow could be approximated as $h_{\mathrm{c}} = 10.42 - v + 10\sqrt{v}$. Since there is only one fan per radiator, it is assumed that the transfer coefficients are similar for both zones. Thus, the thermal inputs from the room to the core and to the coil could be formulated as $q = h_{\mathrm{c}}A_{\mathrm{dr}}(\tau_{\mathrm{r}} - \tau_{\mathrm{d}})$ and $q = h_{\mathrm{c}}A_{\mathrm{ur}}(\tau_{\mathrm{r}} - \tau_{\mathrm{u}})$. Hence, Eq. (1) and Eq. (2) could be updated as Eq. (4) and Eq. (5). Eq. (3) is a special case of Eq. (6) when the fan stops and $u_{\mathrm{fan},k} = 0$.

$$c_{\mathrm{d}} m_{\mathrm{d}}(\tau_{\mathrm{d},k+1} - \tau_{\mathrm{d},k}) = U_{\mathrm{d}} A_{\mathrm{d}}(\tau_{\mathrm{r},k} - \tau_{\mathrm{d},k})\Delta t + U_{\mathrm{u}} A_{\mathrm{u}}(\tau_{\mathrm{u},k} - \tau_{\mathrm{d},k})\Delta t + h_{\mathrm{c}} A_{\mathrm{d}}(\tau_{\mathrm{r},k} - \tau_{\mathrm{u},k})\Delta t \tag{4}$$

$$c_{\mathrm{u}} m_{\mathrm{u}}(\tau_{\mathrm{u},k+1} - \tau_{\mathrm{u},k}) = P_{\mathrm{el,k}}\Delta t - U_{\mathrm{u}} A_{\mathrm{u}}(\tau_{\mathrm{u},k} - \tau_{\mathrm{d},k})\Delta t + h_{\mathrm{c}} A_{\mathrm{u}}(\tau_{\mathrm{r},k} - \tau_{\mathrm{u},k})\Delta t \tag{5}$$

$$\begin{aligned} \begin{bmatrix} \tau_{\mathrm{d},k+1} \\ \tau_{\mathrm{u},k+1} \end{bmatrix} = & \begin{bmatrix} 1 - \frac{U_{\mathrm{d}}A_{\mathrm{d}}\Delta t}{c_{\mathrm{d}}m_{\mathrm{d}}} - \frac{U_{\mathrm{u}}A_{\mathrm{u}}\Delta t}{c_{\mathrm{d}}m_{\mathrm{d}}} - u_{\mathrm{fan},k}\frac{h_{\mathrm{c}}A_{\mathrm{dr}}\Delta t}{c_{\mathrm{d}}m_{\mathrm{d}}} & \frac{U_{\mathrm{u}}A_{\mathrm{u}}\Delta t}{c_{\mathrm{d}}m_{\mathrm{d}}} \\ \frac{U_{\mathrm{u}}A_{\mathrm{u}}\Delta t}{c_{\mathrm{u}}m_{\mathrm{u}}} & 1 - \frac{U_{\mathrm{u}}A_{\mathrm{u}}\Delta t}{c_{\mathrm{u}}m_{\mathrm{u}}} - u_{\mathrm{fan},k}\frac{h_{\mathrm{c}}A_{\mathrm{ur}}\Delta t}{c_{\mathrm{u}}m_{\mathrm{u}}} \end{bmatrix} \begin{bmatrix} \tau_{\mathrm{d},k} \\ \tau_{\mathrm{u},k} \end{bmatrix} \\ & + \begin{bmatrix} 0 \\ \frac{\Delta t}{c_{\mathrm{u}}m_{\mathrm{u}}} \end{bmatrix} P_{\mathrm{el},k} + \begin{bmatrix} \frac{U_{\mathrm{d}}A_{\mathrm{d}}\Delta t}{c_{\mathrm{d}}m_{\mathrm{d}}} + u_{\mathrm{fan},k}\frac{h_{\mathrm{c}}A_{\mathrm{dr}}\Delta t}{c_{\mathrm{d}}m_{\mathrm{d}}} \\ u_{\mathrm{fan},k}\frac{h_{\mathrm{c}}A_{\mathrm{ur}}\Delta t}{c_{\mathrm{u}}m_{\mathrm{u}}} \end{bmatrix} \tau_{\mathrm{r},k} \end{aligned} \tag{6}$$

where $u_{\mathrm{fan},k} \in \{0, 1\}$ denotes the fan's action and it is assumed that the fan's speed is constant. The model structure allows to use the system identification toolbox provided by MATLAB [7][8] to identify the unknown parameters in Eq. (6). Initial guesses and bounds of the unknown parameters need to be calculated and supplied to the toolbox.

3. Results

The data measured in the discharging process are shown in Figure 4. It could be observed that the core temperature goes up after the fan starts. This would not be possible to explain if a first-order model was chosen. The estimated core and coil temperature combining the identified model and a Kalman filter are also shown in Figure 4, which agree well with the measurements.

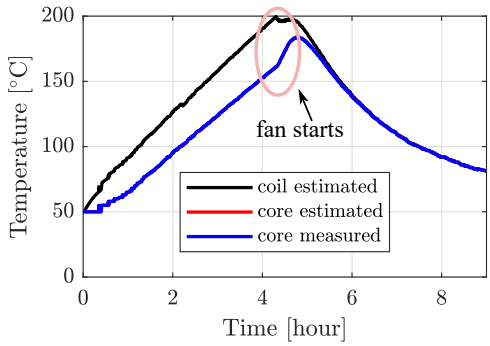

Figure 4: State estimation including charging and discharging process

Table 2: Parameters identified using grey-box modelling technique

Parameter	Value	Unit	Parameter	Value	Unit
$U_{\mathrm{d}}A_{\mathrm{d}}$	0.0066	kW/K	$U_{\mathrm{u}}A_{\mathrm{u}}$	0.0148	kW/K
$c_{\mathrm{d}}m_{\mathrm{d}}$	321.6744	kJ/K	$c_{\mathrm{u}}m_{\mathrm{u}}$	49.3171	kJ/K
Δt	1	s	$h_{\mathrm{c}}A_{\mathrm{dr}}$	0.0064	kW/K
$h_{\mathrm{c}}A_{\mathrm{ur}}$	0.0039	kW/K			

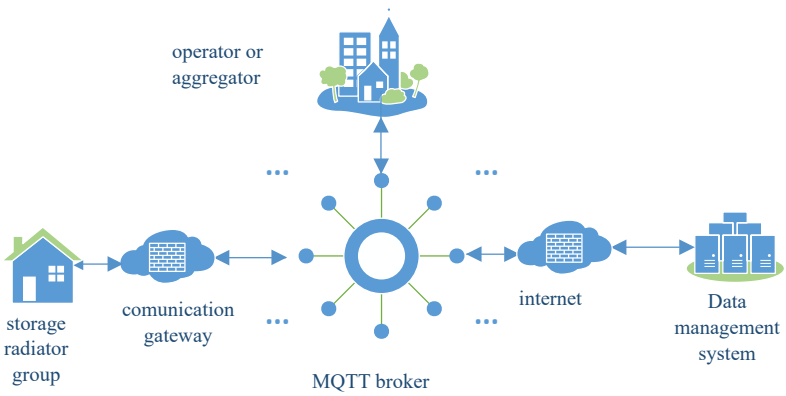

Figure 5: Integration of aggregated storage radiators into existing platform

From the identified state space model, parameters could be separated and are summarized in Table 2. Further separation of the parameters is not possible with existing measurements. Note that, the model becomes time-variant due to fan's action $u_{\mathrm{fan},k}$.

The overall platform to aggregate the radiators and track external set points is illustrated in Figure 5, where the PV installation owner or system operator could set the desired aggregated response and the micro-controller depicted in Figure 3(a) controls the nine radiators according to their energy status. The modelling results in previous sections support the control algorithm design and the experimental results from the week 50 of 2018 are summarised in Figure 6, where the nine storage heaters were aggregated to track external set points. From Figure 6(a), it could be seen that comfort is maintained. Through an analysis of the correlation between time-varying set points and the aggregated response, the activation time is identified to be 15 seconds, as shown in Figure 6(b).

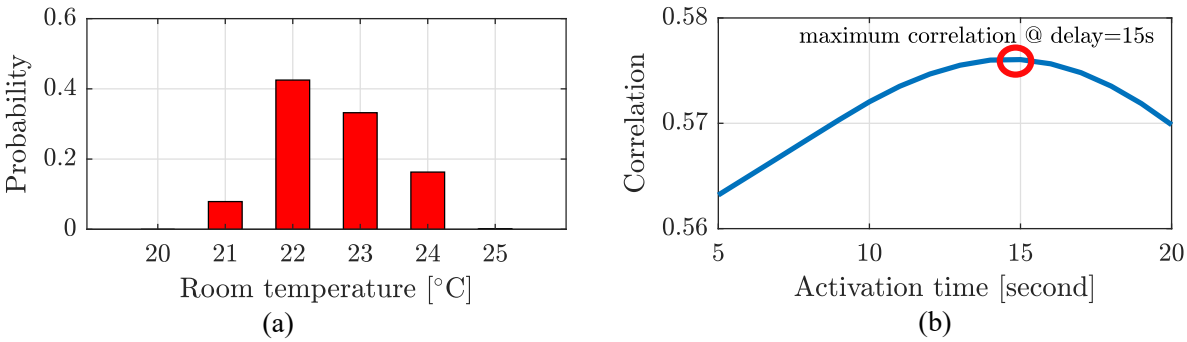

Figure 6: Experimental results. (a): probability distribution of room temperature; (b): correlation between power set points and aggregated response

Hence, the 9 storage radiators have the potential to provide the FNR service of ±11kW with an activation time of 15 seconds and an energy capacity of 167 kWh. The service could be remunerated if 250 storage radiators could be aggregated to provide FNR of 0.3 MW.

4. Conclusion

This paper experimentally evaluates the demand response potential from aggregated high-temperature storage radiators. A dedicated experimental platform was built for this purpose. The methodology consists of grey-box modelling of the charge and discharge processes and aggregating the nine storage radiators to track setpoints sent by external stakeholders with balancing needs.

From the experimental results, it was found out that the aggregated storage radiators have an activation time of 15 seconds and could provide significant energy capacity while the end-users' comfort was maintained. Future work includes demonstrating the coordination between storage radiators and electric battery to balance fluctuating PV production.

Acknowledgments

This research was part of a project which is funded by the Danish EUDP (Energy Technology Development and Demonstration Programme). Project title: EnergyLab Nordhavn - Smart components in integrated energy systems, project number: 64015-0055.

References

[1] J. Raadschelders, F. Sikkema, and B. Groen, "Potential for smart electric thermal storage Contributing to a low carbon energy system," *DNV KEMA Energy & Sustainability*, 2013.
[2] H. Zhao, Q. Wu, S. Hu, H. Xu, and C. N. Rasmussen, "Review of energy storage system for wind power integration support," *Applied Energy*, vol. 137, pp. 545–553, 2015.
[3] H. Hao, D. Wu, J. Lian, and T. Yang, "Optimal coordination of building loads and energy storage for power grid and end user services," *IEEE Transactions on Smart Grid*, 2017.
[4] E. Vrettos, E. C. Kara, J. MacDonald, G. Andersson, and D. S. Callaway, "Experimental demonstration of frequency regulation by commercial buildings-Part II: Results and performance evaluation," *IEEE Transactions on Smart Grid*, 2016.
[5] M. Marinelli, S. Martinenas, K. Knezović, and P. B. Andersen, "Validating a centralized approach to primary frequency control with series-produced electric vehicles," *Journal of Energy Storage*, vol. 7, pp. 63–73, 2016.
[6] H. Cai and S. You, "D4.3b: Design, development and testing of smart controllers for distributed energy resources & D4.3c: Validation document on field-data collection from storage heaters Photo: By," tech. rep., Technical University of Denmark, 2019.
[7] L. Ljung, *Systems Identification: Theory for the User*. Prentice Hall, 1987.
[8] The MathWorks Inc., "System Identification Toolbox." `https://uk.mathworks.com/products/sysid.html`.